



Small fatigue crack growth and failure mode transitions in a Ni-base superalloy at elevated temperature

M.J. Caton^{a,*}, S.K. Jha^b

^a Materials and Manufacturing Directorate, Air Force Research Laboratory (AFRL/RXLMN), Wright-Patterson AFB, OH 45433-7817, USA

^b Universal Technology Corporation, 1270 N. Fairfield Road, Dayton, OH 45432, USA

ARTICLE INFO

Article history:

Received 4 December 2009

Received in revised form 25 January 2010

Accepted 27 January 2010

Available online 2 February 2010

Keywords:

Fatigue

Small crack

Fractography

Intergranular

Transgranular

Dwell

ABSTRACT

A study of the long and small fatigue crack growth behavior in IN100 tested at 650 °C both with and without dwell periods is summarized. A significant small crack effect is evident in this alloy, and it is observed that the influence of loading variables on small crack behavior is profoundly different from that on long cracks. While a 6 s dwell has negligible effect on long crack growth rates, it results in more than an order of magnitude faster growth for small cracks ($\sim 30 \mu\text{m}$ to 1 mm). Long crack growth is dominated by intergranular cracking both with and without 6 s dwell. Small crack growth mode depends on numerous factors including crack size, dwell time, exposure to environment, and character of initiation site. Transitions in small crack growth modes and the operative crack growth mechanisms are discussed.

Published by Elsevier Ltd.

1. Introduction

The current life-management approaches for fracture-critical components in military turbine engines are based on the expected worst-case behavior, where safe life limits are determined from a 1 in 1000 probability of the existence of a crack of detectable size (typically $\sim 800 \mu\text{m}$). These life limits are traditionally established empirically by extrapolating random deviations from the mean lifetime [1]. However, recent studies of turbine engine alloys have shown that the life-limiting behavior is often not accurately predicted by applying random deviations about the mean life, since the worst-case and mean lifetime distributions can frequently result from distinctly different failure mechanisms [2–4]. Therefore, a more accurate prediction of life-limiting behavior is sought through mechanistically-derived probabilistic methods.

Fig. 1 shows an example of fatigue lifetimes previously reported [2] for IN100, a common powder metallurgy (P/M) Ni-base superalloy used in turbine engines. Here it is seen that the trend in the mean lifetime, shown by the dashed lines, is very different from that observed for minimum life specimens. Further, the hatched regions, which indicate the range of predicted life assuming immediate crack initiation, show good agreement with the worst-case failures. This strongly suggests that while the mean life is composed primarily of crack initiation, the minimum life distributions are dominated by crack growth, where the cycles required to initiate

a crack can be considered negligible. Improved accuracy of predicted worst-case life limits can therefore be achieved by characterizing crack growth behavior.

To ensure the accuracy of crack growth-based predictions, it is important to identify the degree to which small crack effects are present under relevant loading conditions. Fig. 2 shows the previously reported [2] crack growth behavior for IN100, under both dwell and no-dwell loading conditions. It is seen that a significant small crack effect is present in this alloy under these conditions. In addition, these data indicate that the effect of modest changes in loading condition (in this case, the application of 6 s dwell time at peak load) can be profoundly different on small crack growth compared to long crack growth behavior. Aside from a slightly higher crack growth threshold seen with 6 s dwell, the long crack data indicate essentially no effect of the dwell time on growth rates. The small crack data in Fig. 2, on the other hand, show a very significant effect of dwell, where growth rates under the dwell condition can be more than an order of magnitude faster for initial crack growth (crack sizes ~ 50 – $250 \mu\text{m}$). The crack growth (CG) life predictions in Fig. 1 include this observed small crack behavior [2].

It is recognized that understanding the early crack growth behavior is critical for developing more accurate, mechanistically-based models of fatigue life limits, thereby enabling safer and more affordable life-management practices. This paper provides a detailed examination of small crack growth behavior in IN100, and the mechanisms that drive the worst-case failures under the loading conditions depicted in Fig. 1.

* Corresponding author. Tel.: +1 937 255 4490.

E-mail address: Michael.Caton@wpafb.af.mil (M.J. Caton).

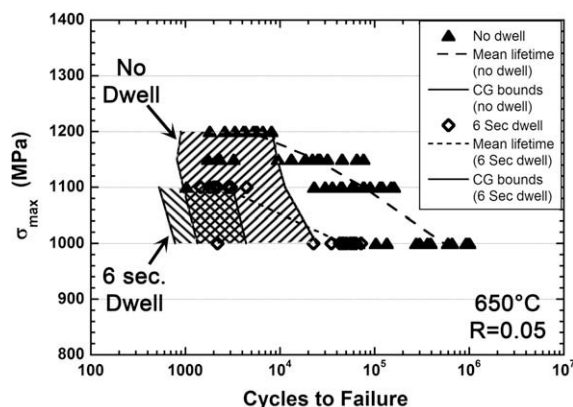


Fig. 1. Previously reported [2] fatigue lifetimes for IN100 tested at 650 °C, 0.33 Hz, $R = 0.05$, and both with and without 6 s dwell at peak load. The hatched regions indicate the predicted range of fatigue crack growth life.

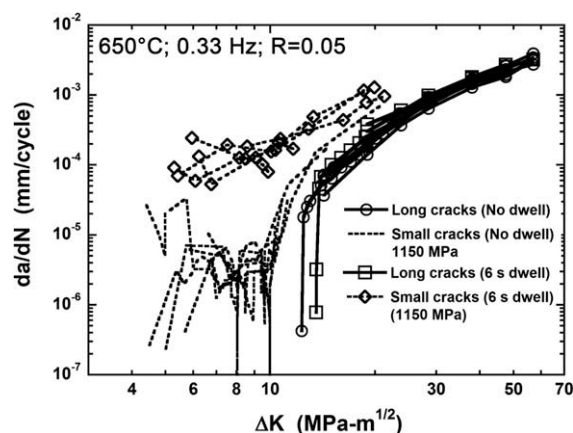


Fig. 2. Previously reported [2] long and small crack growth data for IN100 tested at 650 °C, 0.33 Hz, $R = 0.05$ both with and without 6 s dwell loading.

2. Materials and experimental procedures

The material examined in this paper is a powder-metallurgy (P/M) processed and subsolvus-treated nickel-base superalloy, IN100, which was reported on previously [4]. The microstructure of the alloy consisted of γ -phase grains and primary, secondary, and tertiary γ' precipitates. The average γ grain size was about 3–4 μm and the grain structure was quite equiaxed. In addition to the γ and γ' phases, the microstructure also contained non-metallic particles (NMP) and pores, which are typically contained in powder-processed superalloy materials [5,6]. Note that at least two kinds of NMP were observed, distinguishable by their morphology. One possessed a blocky appearance while the other had a granular, sponge-like morphology. Characteristics of these types of NMP in superalloys have been reported in other studies [5,6]. From the fatigue failure perspective, however, both types were found to be important and, in the given number of experiments, appeared to produce similar crack initiation sizes and range in lifetimes. Throughout the paper, these are referred to generically as NMPs. In general, the NMPs are somewhat larger than the pores, with equivalent diameters of about 20–40 μm , and significantly less prevalent. For more details on the size distributions and volume fractions of the pores and NMP in this alloy, the reader is referred to [4].

The 0.2% yield strength and the ultimate tensile strength of the material at the test temperature of 650 °C were about 1100 and 1379 MPa, respectively. The percent elongation at 650 °C was about 20% and the elastic modulus was about 186 GPa.

The specimens tested in this study were extracted in the circumferential orientation from a pancake forging of the material. A cylindrical, button-head test specimen with a gage length of 15.2 mm and a diameter of 5 mm was used, as described in [7]. The specimens had a low-stress-ground (LSG) finish. The fatigue tests were conducted using an MTS servo-hydraulic test system with a 646 controller. An electric resistance furnace was mounted on the test frame. A high-temperature button-head gripping assembly was used in conjunction with a standard collet-grip system to transfer load to the sample. The hydraulic grip units were water-cooled. Temperature-control thermocouples were welded outside of the specimen gage section to maintain the test temperature at the specimen. The tests were performed in load control at a frequency of 0.33 Hz, a stress ratio (R) of 0.05, and a temperature of 650 °C. The effect of dwell was examined, whereby a series of specimens were tested with a 6 s hold time applied at the peak load. The fracture surfaces of all specimens were examined using scanning electron microscopy to identify and characterize crack initiation sites and crack growth morphology.

Small crack growth rates were monitored for numerous fatigue specimens using a standard replication technique. The gage sections of the small crack specimens were electropolished, typically removing about 10–15 μm of material, and achieving a mirror finish, which facilitated the observation of cracks on the acetate replication tape. The small crack growth tests were periodically interrupted, the specimen was cooled to room temperature, and a replication of the entire surface of the gage section was taken while the specimen was held under a static tensile load of $\sim 70\%$ σ_{max} . Small crack growth rates were calculated using a 3-point sliding polynomial fit to the crack size versus cycle data. The stress intensity factor range, ΔK , was calculated using a solution from Raju and Newman [9] for a surface crack in a rod and assuming a semi-circular crack shape (i.e., depth/half length = $a/c = 1$), and the reported data represents ΔK at the surface tip (i.e., $\phi = 0^\circ$).

Long fatigue crack growth rates were acquired using two different sizes of compact tension, $C(T)$, specimens with nominal height, width, and thickness of 24 mm, 20 mm, and 5 mm, respectively, or 48 mm, 40 mm, and 10 mm, respectively. No difference in crack growth rates was observed between these two $C(T)$ specimen sizes. Long crack tests were conducted at 650 °C, a stress ratio (R) of 0.05, and using a triangle waveform at a frequency of 0.33 Hz, both with and without a 6 s dwell period applied at the peak load. A single threshold test was conducted for both the 6 s dwell and no-dwell loading conditions, following the standard K -decreasing procedure outlined in ASTM Standard E647, where crack size was monitored using direct current potential difference (DCPD) measurements. Additional data were acquired at discrete ΔK levels within the Paris regime of the crack growth curves (ΔK ranging from 14.25 to 57 $\text{MPa}\cdot\text{m}^{1/2}$) using a K_{max} -constant technique to enable the acquisition of a significant amount of data within relatively short times and from relatively few specimens. In this procedure, blocks of constant loading condition are applied for a crack extension adequate to give a steady state growth rate. In this case, individual blocks resulted in approximately 0.3 mm of crack extension. The maximum K levels were always maintained constant or increased from one block of loading to the next to minimize load interaction effects. Data from K_{max} -constant loading were acquired from eight separate specimens.

3. Results and discussion

3.1. Comparing long and small crack growth behavior

Fig. 2 compares the previously reported long and small crack growth rates observed in this alloy under loading both with and

Download English Version:

<https://daneshyari.com/en/article/778520>

Download Persian Version:

<https://daneshyari.com/article/778520>

[Daneshyari.com](https://daneshyari.com)